Preprint LBNL-39895

^{3}He- and ^{4}He-induced nuclear fission – a test of the transition state method*

Th. Rubehn,† K. X. Jing, L. G. Moretto,
L. Phair, K. Tso, and G. J. Wozniak

Nuclear Science Division,
Lawrence Berkeley National Laboratory,
University of California, Berkeley, California 94720, USA

Abstract

Fission in ^{3}He and ^{4}He induced reactions at excitation energies between the fission barrier and 140 MeV has been investigated. Twentythree fission excitation functions of various compound nuclei in different mass regions are shown to scale exactly according to the transition state prediction once the shell effects are accounted for. New precise measurements of excitation functions in a mass region where shell effects are very strong, allow one to test the predictions with an even higher accuracy. The fact that no deviations from the transition state method have been observed within the experimentally investigated excitation energy regime allows one to assign limits for the fission transient time. The precise measurement of fission excitation functions of neighboring isotopes enables us to experimentally estimate the first chance fission probability. Even if only first chance fission is investigated, no evidence for fission transient times larger than 30 zs can be found.

*Talk at the XXXV. International Winter Meeting on Nuclear Physics, Bormio, Italy, 1997 and to be published in the proceedings.

†Electronic address: TRubehn@lbl.gov

1 Introduction

The study of the fission process is – even more than half a century after its discovery – still of general interest. This is caused by both the complexity of the process itself and the availability of new accelerators and techniques that enable the study of new aspects of fission. While several interesting experiments have been performed using relativistic heavy ion beams, we will in this paper concentrate on the investigation of light particle induced nuclear fission at excitation energies between the fission barrier and ∼140 MeV. It has been shown recently that a novel analysis [1, 2, 3] allows for the model-independent extraction of fundamental quantities of the fission process, like effective fission barriers, shell effects, and the much discussed fission delay time [1, 4, 5].

Fission excitation functions vary dramatically from nucleus to nucleus over the periodic table [6, 7, 8]: Some of the differences can be understood in terms of a changing liquid-drop fission barrier with the fissility parameter, others are due to to strong shell effects which occur e.g. in the neighborhood of the double magic numbers Z=82 and N=126. Further effects may be associated with pairing and the angular momentum dependence of the fission barrier [9, 10].

Fission rates have been calculated most often on the basis of the transition state method introduced by Wigner [11], and later applied to fission by Bohr and Wheeler [12]. Recent publications claim the failure of the transition state rates to account for the measured amounts of prescission neutrons or γ rays in relatively heavy fissioning systems [4, 5, 13]. This alleged failure has been attributed to the transient time necessary for the so-called slow fission mode to attain its stationary decay rate [14, 15, 16, 17, 18, 19, 20, 21, 22]. The larger this fission delay time, the more favorably neutron decay competes with the fission process. This leads to an effective fission probability smaller than predicted by the Bohr - Wheeler formula. The experimental methods of these studies, however, suffer from two difficulties: First they require a possibly large correction for post-saddle, but pre-scission emission; second, they are indirect methods since they do not directly determine the fission probability. The measured prescission particles can be emitted either before the system reaches the saddle point, or during the descent from saddle to scission. Only from the anomalies in the first component, would deviations of the fission rate from its transition state value be expected. The experimental separation of

the two contributions, however, is fraught with difficulties which make the evidence ambiguous. As a different ansatz, we will, in this paper, therefore study the validity of the transition state method by directly measuring the fission probability and its energy dependence over a broad energy range. By investigating several old and new data sets, we are able to test the transition state rates for a large number of systems.

2 Experiment

A set of experiments investigating fission excitation functions of various compound nuclei has been performed in the 1960s at Berkeley [8]. All experiments have used mica detectors and have thus required very high beam currents and rather long irradiation times to compensate for the very small angular coverage of the detectors. The data have initially been used for a first test of the method proposed by Moretto *et al.* [1].

In two recent experiments, we have measured fission excitation functions of the compound nuclei ^{200}Tl, ^{211}Po, ^{212}At, and ^{209,210,211,212}Po, formed in the reactions ^{3}He + ^{197}Au, ^{206,207,208}Pb, ^{209}Bi and ^{4}He + ^{206,207,208}Pb, respectively. Both runs have been performed at the Lawrence Berkeley National Laboratory's 88 inch cyclotron which delivered between 19 and 26 different energies per ion species.

To cover a large solid angle and, therefore, to minimize beam time, we performed an experiment using two large area parallel-plate-avalanche counters (PPACs) with an active area of 200 x 240 mm ^{2} each. The detectors were mounted at 80 $^{\circ}$ and 260° with respect to the beam axis, allowing for the detection of both fission fragments in coincidence. The PPACs were placed at a distances of 150 mm from the target to the center of each detector resulting in a coverage of approximately 20% of 4π. The accuracy achieved in these experiments is significantly better than the one of the old runs using mica detectors.

In Fig. 1, we show the experimental fission cross sections for the three compound nuclei ^{200}Tl, ^{211}Po, and ^{212}At as a function of excitation energy. The error bars denote both the statistical and the systematic errors. While the statistical errors dominates at the lowest energy points, the systematic uncertainties are the main contribution at higher excitation energies. Fig. 2 shows the results obtained in a most recent experiment. Here, fission cross sections of the compound nuclei ^{209,210,211,212}Po have been measured in ^{3}He

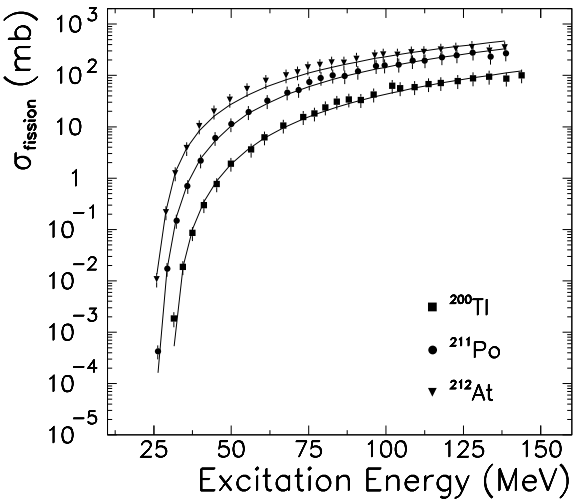

Fig. 1: Excitation function for fission of several compound nuclei formed in ^{3}He induced reactions. The different symbols correspond to the experimental data points. The solid line shows the results of a fit to the data using a level density parameter $a_n = A/8$. The error bars denote the statistical and systematic errors combined in quadrature.

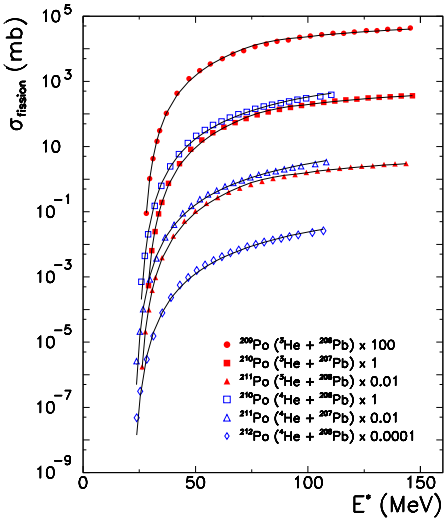

Fig. 2: Same as Fig. 1 for fission of the compound nuclei ^{209,210,211,212} Po formed in ^{3}He and ^{4}He induced reactions.

and ^{4}He induced reactions. The maximum excitation energies are dominated by the K of the cyclotron and the significantly different Q value of the compound nuclei for both projectiles. The observed systematically higher fission probability for the α induced reactions is due to the higher angular momentum of the compound nuclei. The comparison between the data shown in Fig. 1 and those presented in Fig. 2 demonstrates the improvement made in the quality of the measurements [24].

Cross sections were determined for these fission events using

$$\sigma_f = \frac{n_f A}{n_{beam} N_A m} \eta(\theta, \phi), \tag{1}$$

where n_f and n_{beam} are the number of fission events and the number of beam particles, respectively. A represents the mass number of the target, N_A Avogadro's constant, and m the thickness of the target. Due to the incomplete angular coverage, the quantity $\eta(\theta, \phi)$ which accounts for the geometrical acceptance and for the non-isotropic emission of the fission fragments has be be taken into account. The anisotropic angular distribution $\frac{(d\sigma/d\Omega)_\theta}{(d\sigma/d\Omega)_{90^\circ}}$ of the fission fragments has been shown to be reasonably described by the function $\sin^{-1}\theta$ [9]. We have used this dependence for the determination of our acceptance. Comparison between our α induced fission excitation functions and those measuring the angular dependence [8] agree very well.

The excitation energy was calculated assuming a full momentum and mass transfer of the helium ions to the compound nucleus (CN). The binding energies of ^{3}He, the target isotopes, and the compound nuclei were taken from nuclear mass tables [25].

3 Analysis

The experimental data shown above are analyzed according to a rather simple method proposed by Moretto *et al.* [1]. In this section, we briefly reflect the procedure.

Using the transition state expression for the fission decay width

$$\Gamma_f \approx \frac{T_s}{2\pi} \frac{\rho_s(E - B_f - E_r^s)}{\rho_n(E - E_r^{gs})}, \tag{2}$$

the fission cross section can be written as follows:

$$\sigma_f = \sigma_0 \frac{\Gamma_f}{\Gamma_{\text{total}}} \approx \sigma_0 \frac{1}{\Gamma_{\text{total}}} \frac{T_s \rho_s(E - B_f - E_r^s)}{2\pi \rho_n(E - E_r^{gs})}, \tag{3}$$

where σ_0 is the compound nucleus formation cross section, Γ_f is the decay width for fission and T_s is the energy dependent temperature at the saddle; ρ_s and ρ_n are the saddle and ground state level densities, B_f is the fission barrier, and E the excitation energy. Finally, E_r^s and E_r^{gs} represent the saddle and ground state rotational energies.

To further evaluate the expression, we make use of $\rho(E) \propto \exp(2\sqrt{aE})$ for the level density and rewrite Eq. 3 as:

$$\ln\Big(\frac{\sigma_f}{\sigma_0}\Gamma_{\rm total}\frac{2\pi\rho_n(E-E_r^{gs})}{T_s}\Big) = 2\sqrt{a_f(E-B_f-E_r^s)}. \tag{4}$$

Since the neutron width Γ_n dominates the total decay width in our mass and excitation energy regime, we can write:

$$\Gamma_{\rm total} \approx \Gamma_n \approx KT_n^2\frac{\rho_n(E-B_n-E_r^{gs})}{2\pi\rho_n(E-E_r^s)} \tag{5}$$

where B_n represents the binding energy of the last neutron, T_n is the temperature after neutron emission, and $K = \frac{2m_nR^2g'}{\hbar^2}$ with the spin degeneracy $g' = 2$.

The study of the fission process in the lead region forces us to take strong shell effects into account. For the fission excitation functions discussed in this paper, the lowest excitation energies for the residual nucleus after neutron emission are of the order of 15-20 MeV and therefore high enough to assume the asymptotic form for the level density which is given below:

$$\rho_n(E-B_n-E_r^{gs}) \propto \exp\left(2\sqrt{a_n(E-B_n-E_r^{gs}-\Delta_{shell})}\right) \tag{6}$$

where Δ_{shell} is the ground state shell effect of the daughter nucleus $(Z, N-1)$. For the level density at a few MeV above the saddle point, we can use

$$\rho_s(E-B_f-E_r^s) \propto \exp\left(2\sqrt{a_f(E-B_f^*-E_r^s)}\right) \tag{7}$$

since the large saddle deformation implies small shell effects. Deviations due to pairing, however, may be expected at very low excitation energies. In Eq. 7, we introduced the quantity B_f^* which represents an effective fission barrier, or, in other words, the unpaired saddle energy, i.e. $B_f^* = B_f + 1/2g\Delta_0^2$ in the case of an even-even nucleus and $B_f^* = B_f + 1/2g\Delta_0^2 - \Delta_0$ for nuclei

with odd mass numbers. Here, Δ_0 is the saddle gap parameter and g the density of doubly degenerate single particle levels at the saddle.

Finally, the use of Eq. 6 and Eq. 7 for the level densities allows us to study the scaling of the fission probability as introduced in Eq. 4:

$$\frac{1}{2\sqrt{a_n}} \ln\Big(\frac{\sigma_f}{\sigma_0}\Gamma_{\rm total}\frac{2\pi\rho_n(E-E_r^{gs})}{T_s}\Big) = \frac{\ln R_f}{2\sqrt{a_n}} = \sqrt{\frac{a_f}{a_n}(E-B_f^*-E_r^s)}. \qquad (8)$$

The values for B_f^*, Δ_{shell}, and a_f/a_n using $a_n = A/8$ can be obtained by a three parameter fit of the experimental fission excitation functions; the best results of the fits are shown in Figs. 1 and 2. For this procedure, the formation cross sections σ_0, which is approximated by the reaction cross section, and the corresponding values for the maximum angular momentum l_{max} were taken from an optical model calculation.

At high beam energies per nucleon (in particular for the ^{3}He-induced reactions) there might be a significantly contribution from incomplete fusion. We have calculated fusion cross sections by using the Bass model and have used them to estimate the formation cross section σ_0. The fit parameters, however, do only change insignificantly.

4 Results and interpretation

In Fig. 3, we show the shell corrections obtained from the fit to our experimental data. In addition, we also show the results of a similar analysis [1] of fission excitation functions measured in the 1960's. The observed correlation is very good, especially if one reflects how difficult it is to establish a good liquid drop baseline. We point out that the method applied here represents a totally independent way to determine the ground state shell effects.

As pointed out before, plotting the left hand side of Eq. 4 versus the expression $\sqrt{E-B_{\rm f}-E_{\rm r}^{\rm s}}$ should result in a straight line if the transition state predictions hold. In Fig. 4, we show the results for a large number of fission excitation functions. A remarkable straight line can be observed for all compound nuclei investigated. It should be noted that the scaling extends over six orders of magnitude in the fission probability although shell effects are very strong for several nuclei. A fit to the data results in a straight line that goes through the origin and has a slope that represents $a_{\rm f}/a_{\rm n}$, consistent with unity. The observed scaling and the lack of deviations indicates that the transition state rates hold well.

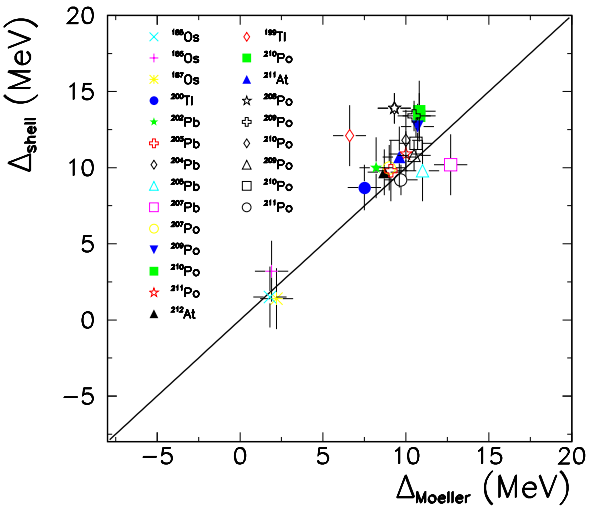

Fig. 3: Shell corrections for the daughter nuclei, extracted from fits to the fission excitation functions plotted against the values determined from the ground state masses.

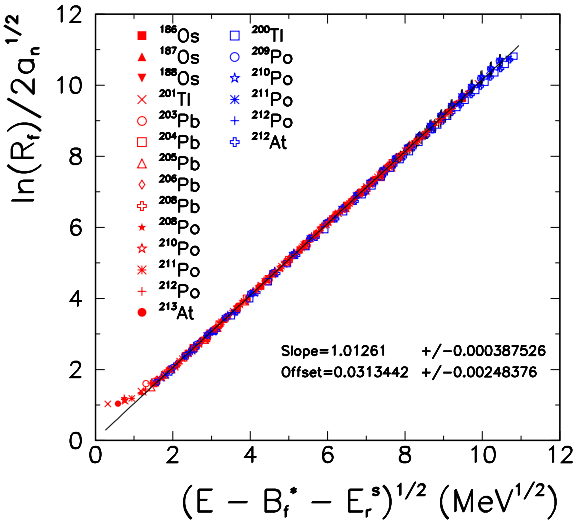

Fig. 4: The quantity $\frac{\ln R_f}{2\sqrt{a_n}}$ vs the square root of the intrinsic excitation energy over the saddle for fission of several compound nuclei as described in the text. The straight line represents a fit to the entire data set.

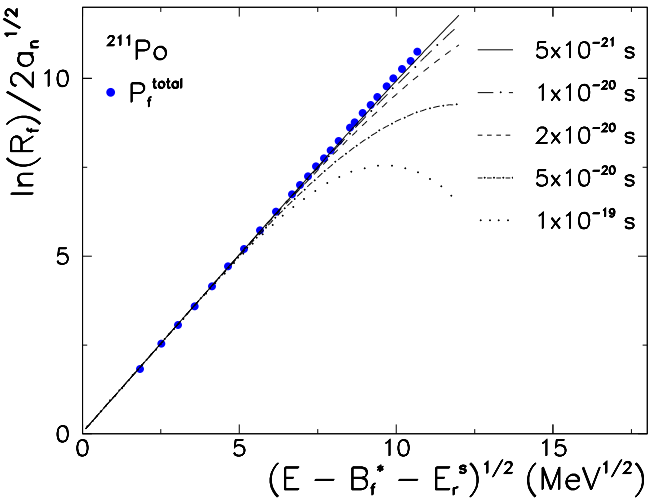

Fig. 5: Same as Fig. 4 for ^{211}Po. The lines represent calculations assuming that no fission occurs during a given transient time which is indicated in the figure. For further details see text.

The excitation energy range covered by the experiments presented here correspond to life times of the compound nuclei between 10^{-18} and 10^{-22} s and should therefore be sensitive to delay times in the fission process. To investigate this effect, we assume a step function for the transient time effects. In this assumption, the fission width can be written as follows:

$$\Gamma_f = \Gamma_f^{\infty} \int_0^{\infty} \lambda(t) \exp(\frac{-t}{\tau_{CN}}) d(\frac{t}{\tau_{CN}}) = \Gamma_f^{\infty} \exp(\frac{-\tau_D}{\tau_{CN}}) \qquad (9)$$

where the quantity $\lambda(t)$ jumps from 0 at times smaller than the transient time τ_D to 1 for times larger than τ_D. Furthermore, Γ_f^{∞} denotes the transition state fission decay width and τ_{CN} represents the life time of the compound nucleus. This expression for the fission decay width has been used in the formalism described above; the parameters B_f^*, Δ_{shell}, and a_f/a_n have been taken from the fit. In Fig. 5, we show the results of these calculations for the compound nucleus ^{211}Po; the different lines indicate different assumed values of the transient time between 1×10^{-19} and 5×10^{-21} seconds. The calculated values show an obvious deviation from the experimental data for assumed transient times larger than 10^{-20} seconds.

In the formalism above, we have only accounted for first chance fission while for the experimental data, we have used the total fission probability. At low excitation energies, first chance fission will certainly be the most dominant contribution. However, at the highest energies higher chance fission is expected to become more and more important. In the following, we shall thus estimate the percentage of first chance fission from our experimental data.

To extract first chance fission from experimental data, we have measured fission excitation functions of neighboring Po isotopes. The difference in the fission probability determines the 1st chance fission probability. Since the energy dependence of the first chance fission probability is determined by subtracting similar cross sections of the two neighboring isotopes, it is essential to measure the cumulative cross sections with high precision; we have discussed this in detail in Ref. [24]. The data measured in a recent experiment (see Fig. 2) should be precise enough to determine the 1st chance fission probability.

First chance fission at a given excitation energy E^* can be determined by subtracting the fission probabilities of two neighboring isotopes:

$$P_f^{1st} = \frac{\left(P_f^{tot}(E^*)\right)_{N,Z} - \left(P_f^{tot}(E^* - S_n - 2T)\right)_{N-1,Z}}{1 - \left(P_f^{tot}(E^* - S_n - 2T)\right)_{N-1,Z}}. \qquad (10)$$

Here, S_n represents the separation energy of the last neutron and T is the temperature of the daughter nucleus given by $T = \sqrt{E^*/a_n}$. We note that the angular momentum dependence is neglected in this simple ansatz. The average angular momentum taken away by one neutron can be estimated to be smaller than $0.5\hbar$.

In Fig. 6, we show the preliminary results of this analysis for ^{4}He induced reactions. At excitation energies smaller than $\sim$45 MeV, 1st chance fission accounts for practically all fission events. However, at higher excitation energies, multi-chance fission sets in and 1st chance fission only accounts for $\sim$10% of the total fission probability at the highest excitation energies investigated. It is interesting that 2nd chance fission becomes even slightly stronger than 1st chance fission around 100 MeV.

As pointed out before, the formalism described in Section 3 has been established for first chance fission only. We thus apply the method to our

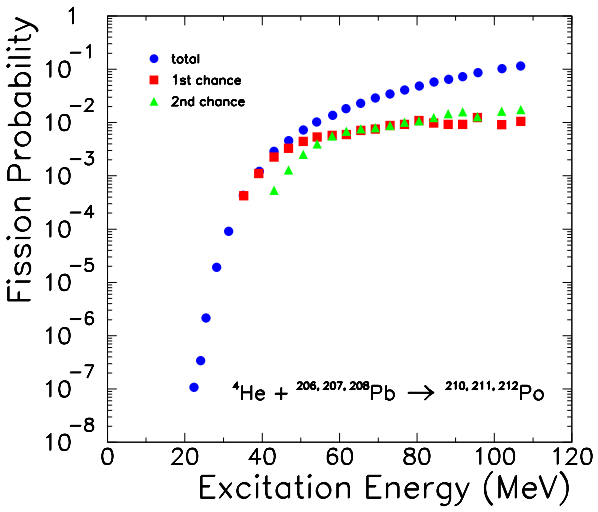

Fig. 6: **PRELIMINARY** first and second chance fission probability for the reaction ^{4}He + ^{206,207,208}Pb.

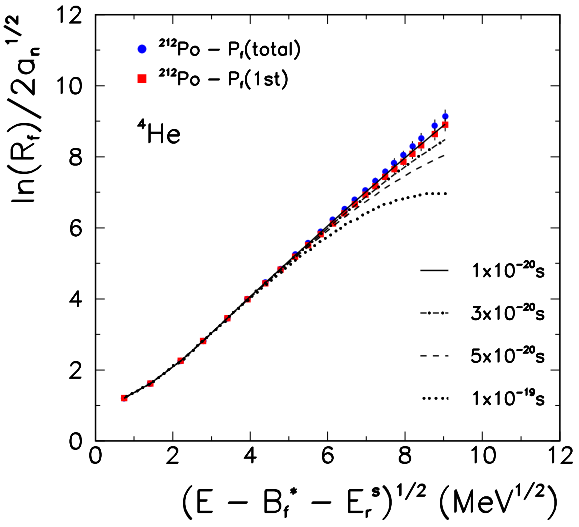

Fig. 7: **PRELIMINARY.** Same as Fig. 5 but for first chance fission of ^{212}Po only.

experimental 1st chance fission results. In Fig. 7, we show the results of this analysis in comparison with the results using the total fission probability. Although there is a small difference between the data investigating 1st chance fission only and those including higher chance fission at high excitation energies, no significant deviations from the straight line are visible. Similar results have been obtained for ^{3}He induced fission. We thus conclude that no deviations from the transition state rates have been found and that fission transient times must be shorter than 30 zs. It seems likely that that any excess prescission emission occurs during the descent from saddle to scission. If this is the case, then the present fission results are not in contradiction with recent measurements of prescission neutron and γ rays [4, 5, 13].

5 Summary

We have measured ^{3}He and ^{4}He induced fission excitation functions. The model-independent analysis of these experimental results allows for the test of the validity of the transition state rates. It furthermore allows one to determine effective fission barriers and the ground state shell effects of the compound nuclei investigated. No deviations from the transition state rate predictions have been observed in our data. Good agreement between the extracted shell corrections and those obtained from the ground state masses have been found. Since the experimental fission rates are well described by the transition state rates and an upper limit for the fission transition time of 30 zs could be determined, it seems likely that any excess prescission emission occurs during the descent from saddle to scission.

Acknowledgement
This work was supported by the Director, Office of Energy Research, Office of High Energy and Nuclear Physics, Nuclear Physics Division of the US Department of Energy, under contract DE-AC03-76SF00098.

References

[1] L.G. Moretto, K.X. Jing, R. Gatti, R.P. Schmitt, and G.J. Wozniak, Phys. Rev. Lett. **75**, 4186 (1995).

[2] Th. Rubehn, K.X. Jing, L.G. Moretto, L. Phair, K. Tso, and G.J. Wozniak, Phys. Rev. C 54, 3062 (1996).

[3] Th. Rubehn, K.X. Jing, L.G. Moretto, L. Phair, K. Tso, G.J. Wozniak, Advances in Nuclear Dynamics 2, Proceedings of the 12th Winter Workshop on Nuclear Dynamics, Snowbird, Utah, 1996, p. 129 (Plenum).

[4] D. Hilscher and H. Rossner, Ann. Phys. Fr. **17**, 471 (1992).

[5] P. Paul and M. Thoennessen, Ann. Rev. Nucl. Part. Sc. **44**, 65 (1994).

[6] G. M. Raisbeck and J.W. Cobble, Phys. Rev. **153**, 1270 (1967).

[7] L.G. Moretto, S.G. Thompson, J. Routti, and R.C. Gatti, Phys. Lett. **38B**, 471 (1972).

[8] A. Khodai-Joopari, Ph.D. thesis, University of California at Berkeley, 1966.

[9] R. Vandenbosch, J.R. Huizenga, *Nuclear Fission* (Academic Press, New York, 1973) and references therein.

[10] C. Wagemans, *The Nuclear Fission Process* (CRC Press, Boca Raton - Ann Arbor - Boston - London, 1991) and references therein.

[11] E. Wigner, Trans. Faraday Soc. **34**, 29 (1938).

[12] N. Bohr and J.A. Wheeler, Phys. Rev. **56**, 426 (1939).

[13] M. Thoennessen and G.F. Bertsch, Phys. Rev. Lett. **71**, 4303 (1993).

[14] P. Grangé and H.A. Weidenmüller, Phys. Lett. **B96**, 26 (1980).

[15] P. Grangé, L. Jun-Qing, and H.A. Weidenmüller, Phys. Rev. C **27**, 2063 (1983).

[16] H.A. Weidenmüller and Z. Jing-Shang, Phys. Rev. C **29**, 879 (1984).

[17] P. Grangé, S. Hassani, H.A. Weidenmüller, A. Gavron, J.R. Nix, and A.J. Sierk, Phys. Rev. C **34**, 209 (1986).

[18] L. Zhongdao, Z. Jingshang, F. Renfa, and Z. Yizhong, Z. Phys. A **323**, 477 (1986).

[19] Z.-D. Lu, B. Chen, J.-S. Zhang, Y.-Z. Zhuo, and H.-Y. Han, Phys. Rev. C **42**, 707 (1990).

[20] D. Cha and G.F. Bertsch, Phys. Rev. C **46**, 306 (1992).

[21] P. Fröbrich, I.I. Gontchar, and N.D. Mavlitov, Nucl. Phys. A **556**, 281 (1993).

[22] K. Siwek-Wilczyńska, J. Wilczyński, R.H. Siemssen, and H.W. Wilschut, Phys. Rev. C **51**, 2054 (1995).

[23] R.H. Iyer, A.K. Pandey, P.C. Kalsi, and C. Sharma, Phys. Rev. C **44**, 2644 (1991).

[24] Th. Rubehn, G.J. Wozniak, L. Phair, L.G. Moretto, and Kin M. Yu, Nucl. Instr. Meth. A (in print),
Preprint LBNL 39398 and LANL e-print nucl-ex/9609004.

[25] G. Audi and A.H. Wapstra, Nucl. Phys. A **565**, 1 (1993).